Atmos. Meas. Tech., 7, 743–755, 2014
www.atmos-meas-tech.net/7/743/2014/
doi:10.5194/amt-7-743-2014

Atmospheric Measurement Techniques
Open Access

Tunable diode laser in-situ CH_4 measurements aboard the CARIBIC passenger aircraft: instrument performance assessment

C. Dyroff[1], A. Zahn[1], S. Sanati[1], E. Christner[1], A. Rauthe-Schöch[2], and T. J. Schuck[2,*]

[1]Karlsruhe Institute of Technology (KIT), Institute of Meteorology and Climate Research (IMK-ASF), Karlsruhe, Germany
[2]Max Planck Institute for Chemistry (Otto Hahn Institute), Mainz, Germany
[*]now at: NRW State Agency for Nature, Environment and Consumer Protection, Recklinghausen, Germany

Correspondence to: C. Dyroff (christoph.dyroff@kit.edu)

Received: 30 September 2013 – Published in Atmos. Meas. Tech. Discuss.: 29 October 2013
Revised: 24 January 2014 – Accepted: 6 February 2014 – Published: 13 March 2014

Abstract. A laser spectrometer for automated monthly measurements of methane (CH_4) mixing ratios aboard the CARIBIC passenger aircraft is presented. The instrument is based on a commercial Fast Greenhouse Gas Analyser (FGGA, Los Gatos Res.), which was adapted to meet the requirements imposed by unattended airborne operation. It was characterised in the laboratory with respect to instrument stability, precision, cross sensitivity to H_2O, and accuracy. For airborne operation, a calibration strategy is described that utilises CH_4 measurements obtained from flask samples taken during the same flights. The precision of airborne measurements is 2 ppb for 10 s averages. The accuracy at aircraft cruising altitude is 3.85 ppb. During aircraft ascent and descent, where no flask samples were obtained, instrumental drifts can be less accurately determined and the uncertainty is estimated to be 12.4 ppb. A linear humidity bias correction was applied to the CH_4 measurements, which was most important in the lower troposphere. On average, the correction bias was around 6.5 ppb at an altitude of 2 km, and negligible at cruising flight level. Observations from 103 long-distance flights are presented that span a large part of the northern hemispheric upper troposphere and lowermost stratosphere (UT/LMS), with occasional crossing of the tropics on flights to southern Africa. These accurate data mark the largest UT/LMS in-situ CH_4 dataset worldwide. An example of a tracer-tracer correlation study with ozone is given, highlighting the possibility for accurate cross-tropopause transport analyses.

1 Introduction

Atmospheric methane (CH_4) is the second-strongest long-lived anthropogenically influenced greenhouse gas (GHG) after carbon dioxide (CO_2) (Solomon et al., 2007). It is most active via its radiative forcing in the upper troposphere and lowermost stratosphere (UT/LMS) (Riese et al., 2012). CH_4 mostly originates from biogenic sources, e.g. wetlands, rice agriculture, biomass burning and ruminant animals (Dlugokencky et al., 2009; Bloom et al., 2010). Anthropogenic CH_4 sources, which account for ~ 60 % of the total source strength, include various industrial processes, e.g. fossil fuel mining and distribution. The emission rate is highly variable (Heimann, 2011) and in particular the future emission rates of wetlands, permafrost and oceanic methane hydrates are highly uncertain (Heimann, 2010; O'Connor et al., 2010).

Global measurements of CH_4 thus serve various purposes: (1) to better constrain the global CH_4 budget and atmospheric trend, (2) to better quantify the different CH_4 sources and assess their future evolution, but (3) also as a transport tracer of tropospheric air to study exchange processes in the UT/LMS. Satellite measurements of CH_4 have been performed with various satellite-borne instruments in recent years (Schneising et al., 2009; Payan et al., 2009; Xiong et al., 2010; Wecht et al., 2012; Worden et al., 2012). While these data are provided on a global scale, they cannot resolve small-scale variability of CH_4 in the UT/LMS. To study these processes, in-situ measurements with high spatial resolution are inevitable.

CH_4 has been measured in-situ during various airborne field campaigns (see e.g. Collins et al., 1993; Spackman et al., 2007; Chen et al., 2010; O'Shea et al., 2013). Regular CH_4 in-situ measurements in the UT/LMS, however, have not been performed yet. Until today, only flask samples were regularly collected aboard aircraft and later analysed in the laboratory for their CH_4 mixing ratio in the framework of the CONTRAIL (Machida et al., 2008) and CARIBIC projects (Brenninkmeijer et al., 2007; Schuck et al., 2012, see also: www.caribic-atmospheric.com). In CARIBIC (Civil Aircraft for the Regular Investigation of the atmosphere Based on an Instrument Container), 15 such air samples per flight were obtained between 2004 and 2009. After a major modification and extension of the instrumentation of the CARIBIC container, altogether 116 air samples were collected during four consecutive long-distance flights per month. The CH_4 mixing ratio was determined by laboratory measurements with high accuracy after each flight sequence (Schuck et al., 2009).

The spatial resolution of these flask data is still modest, and continuous in-situ measurements of the CH_4 mixing ratio are highly valuable in order to better capture the atmospheric variability with a resolution of about a kilometre. Diode-laser absorption spectroscopy offers the capability for precise and accurate measurements at small instrument size, and several research instruments have been developed in the past. They have provided in-situ measurements in the laboratory (Weibring et al., 2010), field (Werle and Kormann, 2001; Nelson et al., 2004), and aboard balloon and aircraft platforms (Scott et al., 1999; Richard et al., 2002; Durry et al., 2002; Gurlit et al., 2005; Berman et al., 2012). In recent years, commercial instruments have become available for laboratory or ground-based field measurements (Crosson, 2008; Chen et al., 2010; Tuzson et al., 2010). However, for the fully automated application aboard civil aircraft, these instruments need to be strongly modified to fulfill the strict safety requirements for unattended operation and to reliably work under strong temperature variations of more than 20 K.

In this paper we present an airborne diode-laser spectrometer, which is based on a commercial Fast Greenhouse Gas Analyser (FGGA, Los Gatos Research). The modifications towards unattended employment aboard passenger aircraft are described. Laboratory tests were performed to determine the spectrometer precision, cross sensitivity to H_2O, and accuracy. A calibration procedure based on the aforementioned flask sample measurements was developed and is presented in detail. The precision and accuracy of airborne in-situ CH_4 measurements during 103 intercontinental flights is analysed and cumulates in a total error estimate. Some illustrative examples of the observations are presented.

2 Instrument setup

The present instrument is based on a commercial Fast Greenhouse Gas Analyser (FGGA[1], Los Gatos Research), which measures CH_4, CO_2, and H_2O mixing ratios based on off-axis integrated cavity output spectroscopy (OA-ICOS) (Baer et al., 2002). We decided for this technique mainly because it provides a rather simple and very rugged optical system, which is an important aspect for unattended airborne employment at conditions of vibration and temperature changes.

In the FGGA, two lasers are used to separately measure CH_4 and H_2O as well as CO_2 in an interleaved fashion. In the present paper, we focus on the CH_4 measurements, as in the CARIBIC project CO_2 is measured with superior precision and accuracy by another in-situ instrument (LI-COR 6252, Lincoln, Nebrasca, USA).

The OA-ICOS technique employed in this instrument is reviewed briefly. The beam of a fibre-pigtailed near infrared (NIR) tunable diode laser emitting around $\nu_0 = 6057.5\,\mathrm{cm}^{-1}$ ($\lambda = 1651\,\mathrm{nm}$) is collimated and guided into an optical cavity formed by two mirrors with reflectivity $R \sim 0.99992$. The beam enters the cavity through the front mirror in an off-axis alignment. In contrast to on-axis alignment, where only the fundamental cavity mode is excited, this approach excites many cavity modes and yields a quasi-continuous transmission spectrum, i.e. the cavity is assumed non-resonant (Sayres et al., 2009). Residual cavity modes are minimised by dithering the distance between the cavity mirrors using piezo electric actuators connected to the front mirror.

Due to the high mirror reflectivity, the residence time τ_{RD} of the photons traversing at the speed of light c inside the cavity, and thus the effective optical pathlength l_{eff} is long compared to single or multipass absorption cells. In our particular case we obtain $\tau_{\mathrm{RD}} \sim 10\,\mu\mathrm{s}$ on average, which corresponds to $l_{\mathrm{eff}} = 3\,\mathrm{km}$ in a $L = 25\,\mathrm{cm}$ long cavity, during which interaction of photons and CH_4 molecules can occur

$$\tau_{\mathrm{RD}} = \frac{l_{\mathrm{eff}}}{c} = \frac{L}{c(1-R)}. \quad (1)$$

The laser radiation leaking out of the rear cavity mirror is collected and focused on a room-temperature InGaAs photodiode with a $\varnothing = 2\,\mathrm{mm}$ active area via a $\varnothing = 50\,\mathrm{mm}$ biconvex lens. Employing laser-wavelength scanning by modulating the laser-injection current, absorption spectra (Fig. 2) are obtained in $\sim 5\,\mathrm{ms}$ and upon averaging are evaluated at 1 Hz with a duty cycle of 0.5. The spectral scan includes two isolated CH_4 absorption features and one H_2O absorption line. The main CH_4 absorption feature ($\nu_0 \approx 6057.1\,\mathrm{cm}^{-1}$, $S_{ij} = 1.2 \times 10^{-21}\,\mathrm{cm\,molec.}^{-1}$) is an unresolved superposition of four individual lines, and the weaker feature ($\nu_0 \approx 6057.5\,\mathrm{cm}^{-1}$, $S_{ij} = 4.5 \times 10^{-23}\,\mathrm{cm\,molec.}^{-1}$) comprises two

[1]This FGGA was originally purchased in 2005 as Fast Methane Analyser, model # 907-0001-1001, which was upgraded in 2008 to a FGGA.

unresolved lines (Rothman et al., 2009). The H_2O line ($\nu_0 \approx 6057.8\,\mathrm{cm}^{-1}$, $S_{ij} = 7.4 \times 10^{-26}\,\mathrm{cm\,molec.}^{-1}$) is rather weak and allows for humidity measurements with relatively low precision.

For our airborne instrument, we use the data processing unit provided with the commercial FGGA. This unit performs all necessary tasks, such as scanning the laser wavelength, acquiring the spectra, and performing a spectral fit to obtain the CH_4 mixing ratio. Fit results along with the cavity pressure, gas temperature, and the ringdown time τ_{RD} are transferred via RS232 serial connection to the housekeeping computer for storage. Unfortunately, with this model version of the FGGA it is not possible to store the measured spectra for post processing or archiving. This important feature may be possible with later FGGA versions, though.

For the employment onboard aircraft, the original instrument was modified to be operated unattended and to fulfill the safety requirements imposed by civil aviation. All parts of the instrument are mounted inside a lightweight, aircraft certified 19-inch rack (enviscope, Germany). A schematic of the instrument is depicted in Fig. 1.

A custom developed power-supply unit comprising commercial DC/DC converters (Mini series DC/DC, Vicor) was implemented to reduce size and weight. For noise-critical components, such as the photodetector and laser driver unit, the supply voltages are filtered to suppress noise and ripple. Before and after instrument modification, the noise characteristics of the Indium Gallium Arsenide (InGaAs) photodiode and subsequent transimpedance amplifier ($G = 3 \times 10^6$ V/W, $\Delta f = 100$ kHz) were studied. The detector-dark noise was measured to be $1.74 \times 10^{-12}\,\mathrm{W\,(Hz)}^{-1/2}$, i.e. practically identical to the value achieved with the original power supply. This dark noise is the dominating noise contribution to the signal-to-noise ratio in OA-ICOS (Dyroff, 2011).

A control computer (V25, Max Planck Institute Mainz, Germany) was installed for housekeeping tasks such as pressure and temperature control.

In the CARIBIC Airbus 340–600 aircraft, an inlet system is permanently installed at the lower fuselage in front of the wing section (Brenninkmeijer et al., 2007). Air is sampled through a sideways facing PFA tube with 12 mm inner diameter at a flow rate of ~ 80 vol-L min^{-1} (volumetric flow rate). The major part of this flow is bypassing the instruments for fast flushing of the inlet line, thus maximising the response to atmospheric variability (see Sect. 4.5).

A flow of 4 sLpm (sLpm = standard liters per minute) is picked off of the main flow and is guided through the FGGA using a piston pump (8006ZV DC, Gardner Denver Thomas GmbH, Germany) located downstream of the OA-ICOS cavity (Fig. 1). A 1 L buffer volume downstream of the cavity minimises pressure fluctuations in the cavity due to the pump strokes. Upstream of the cavity, a proportional valve (Fluid Automation Systems GmbH, model EQI-FIL) is used to establish a constant pressure of 180 ± 0.05 hPa (FGGA standard setting) within the cavity. The flow is measured using a flow meter downstream of the cavity.

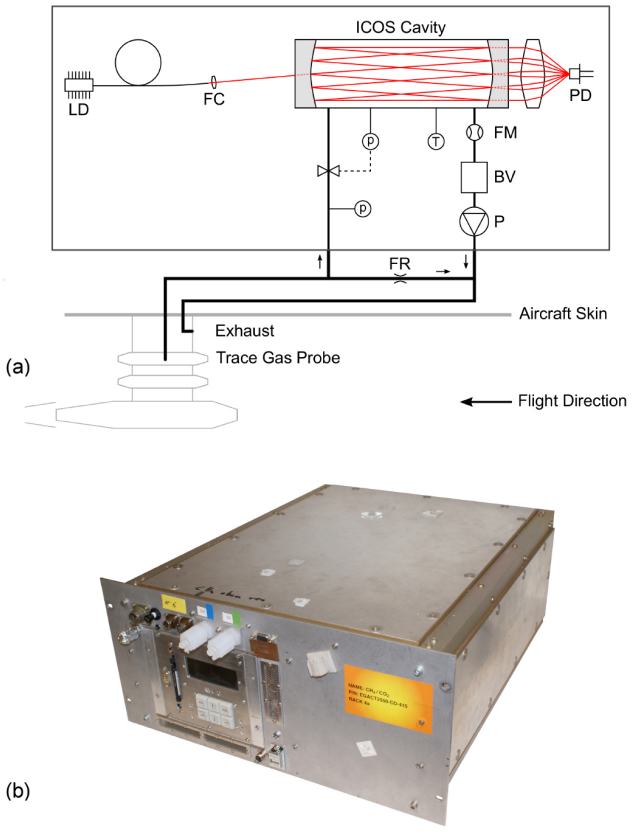

Fig. 1. (a) Schematic setup of the airborne FGGA deployed aboard CARIBIC (additional laser for CO_2 measurements not shown). LD: laser diode, FC: fiber collimator, PD: photo detector, PV: proportional valve, p: pressure sensor, T: temperature sensor, FM: flow meter, BV: buffer volume, P: pump, FR: flow restrictor. **(b)** Photograph of the modified FGGA.

In contrast to the commercial FGGA device, the OA-ICOS cavity and laser coupling optics are thermally insulated by highly efficient insulation material (model va-Q-vip, va-Q-tec, Germany) and are temperature controlled to 40 °C using resistive heaters in combination with software PID controllers of the V25 computer.

The instrument is remotely controlled via the CARIBIC container master computer, which sets it into measurement mode when the aircraft is above the 750 hPa pressure level (2 km standard altitude).

3 Laboratory performance

Prior to the implementation into the CARIBIC payload as well as periodically between flights, the instrument performance was checked in the laboratory. Tests included those for instrument precision, calibration with known CH_4 standards, and determination of the cross sensitivity of the CH_4

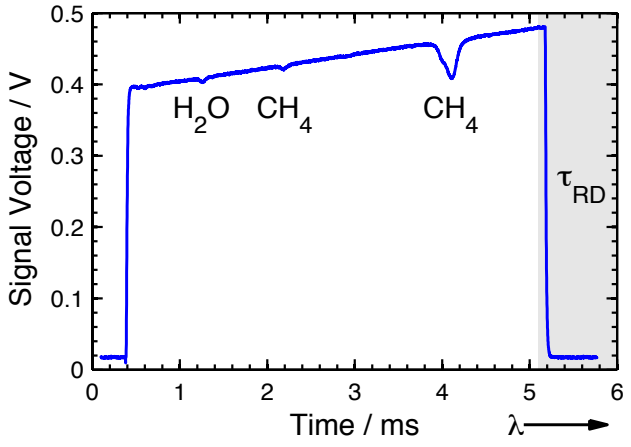

Fig. 2. OA-ICOS cavity transmission spectrum recorded with an oscilloscope showing the CH_4 and H_2O absorption lines probed. The shaded area indicates the time where the ringdown-time constant τ_{RD} is determined.

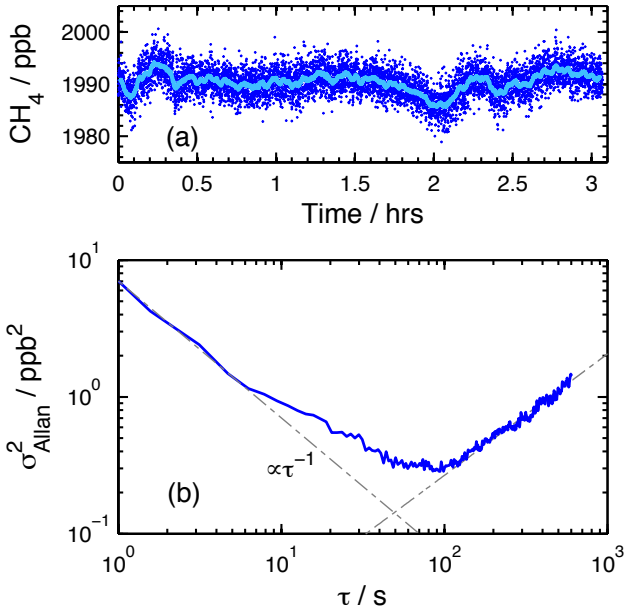

Fig. 3. (a) Time series of a $CH_4 = 1986.8$ ppb gas-standard measurement in the laboratory. The thick line indicates a 80 s moving average. **(b)** Allan variance versus integration time of the time series. The maximum stability time is around 80 s, where the precision of the instrument is $\sigma \sim 0.6$ ppb.

measurements to the water vapour mixing ratio. The respective methods and results obtained are discussed below.

3.1 Precision

In order to determine the precision of the modified FGGA measurements of constant CH_4 mixing ratio from a certified gas standard (Basi Gase, Rastatt, Germany) were performed. This gas standard contained a dry synthetic air mixture with $CH_4 = 1986.8 \pm 1.16$ ppb [NOAA04 Scale, 1 ppb = 1 nmol mol^{-1}, Dlugokencky et al. (2005); Schuck et al. (2009)]. At this mixing ratio, the fractional absorbance is around 11 % or 3.6×10^{-7} cm^{-1} when normalised to the effective optical pathlength of 3 km inside the cavity. The CH_4 mixing ratio was confirmed using gas chromatography at the Max-Planck Institute in Mainz.

The gas standard was provided to the FGGA in a continuous flow, and the CH_4 mixing ratio was obtained at 1 Hz sampling frequency. From the corresponding CH_4 time-series (Fig. 3a) the Allan variance σ^2_{Allan} (Fig. 3b) was obtained by calculating the variance of the differences between adjacent measurements of averaging time τ (Werle et al., 2004; Werle, 2011). With increasing averaging time τ, σ^2_{Allan}, which is an indicator of measurement precision, is reduced. For statistically independent measurements (constant noise spectral density, white noise) one expects a reduction of σ^2_{Allan} proportional to τ^{-1} as indicated by the theoretical dashed line. The measured Allan plot deviates from this line after 6 s, but it is still improved by averaging for up to $\tau_{\text{opt}} \sim 80$ s. When averaging for longer than 80 s, low frequency disturbances (instrumental drift) become dominant, and σ^2_{Allan} is increasing again. Hence, an improvement of precision is not possible by averaging any longer than τ_{opt}. For $\tau = 1$ s averaging we obtain from the Allan plot a precision of $\sigma_{\text{Allan}} = 2.65$ ppb, which corresponds to a fractional absorbance of 5.1×10^{-10} cm^{-1}. The FGGA in-flight data are reported as 10 s averages, where the precision in the laboratory is determined to be $\sigma_{\text{Allan}} = 0.96$ ppb (absorbance 1.9×10^{-10} cm^{-1}). The best precision is found to be $\sigma_{\text{Allan}} = 0.56$ ppb (absorbance 1.07×10^{-10} cm^{-1}) at $\tau_{\text{opt}} \sim 80$ s.

The results obtained in the laboratory are very similar to what we have determined with the unmodified instrument, where the precision was around 2.2 ppb for 1-sec average data. Using an unmodified Fast Methane Analyser (FMA, Los Gatos Research), which relies on the same measurement principle as the FGGA, Tuzson et al. (2010) have determined a precision of ~ 1 ppb for 1 s and ~ 0.14 ppb for 10 s averaging. This is somewhat better than the precision of the present instrument, while the stability time of this FMA was limited to ~ 30 s. We attribute the somewhat better precision found by Tuzson et al. (2010) partially to the fact that our instrument takes CH_4 measurements with a duty cycle of 0.5 as also CO_2 measurements are performed (yet not evaluated) using a second laser. This duty cycle reduction should limit the precision by a factor of $\sqrt{2}\times$. The longer stability time of the present instrument may be attributed to a better thermal stability of our modified FGGA. Note that in contrast to the original FGGA, we maintain the OA-ICOS cavity at a constant temperature.

3.2 Accuracy

The instrument accuracy is affected by multiple factors. A nonlinear or biased instrument function can lead to errors at mixing ratios largely different to the calibration mixing ratio. Instrumental drift can reduce the accuracy of measurements taken long after the instrument stability time derived in an Allan-variance analysis.

We have determined the accuracy of the FGGA in the laboratory by taking measurements of two different calibration standards (standard # 1: 1986.8 ± 1.16 ppb, standard # 2: 1794.3±0.81 ppb). Each of the standards was provided to the inlet of the instrument for 2 min, after which a valve was used to rapidly switch to the other standard (Fig. 4a). This procedure was repeated for 60 min. The measurement sequence was started with a calibration of the FGGA with the calibration routine of the commercial FGGA using standard # 1. For each 2-min sample measurement the average $\langle(CH_4)_{sample}\rangle$ was calculated.

The average mixing ratio derived for standard # 1 is 1982.9 ± 2.1 ppb, and for standard # 2 it is 1787.8 ± 2.1 ppb. Over the 60 min period we thus were able to measure the two standards with an uncertainty of 6.5 ppb (< 0.5 %) using the single-point calibration provided by the FGGA software.

Two observations were made when comparing the individual averages $\langle(CH_4)_{sample}\rangle$ and their respective standard $(CH_4)_{standard}$

$$\Delta_S(CH_4) = \langle(CH_4)_{sample}\rangle - (CH_4)_{standard}. \quad (2)$$

(1) Instrumental drift is the largest source of uncertainty for this measurement, as the FMA measurements drift towards lower mixing ratios (Fig. 4b). (2) Standard # 2 is generally slightly more underestimated by the FGGA. This suggests that the calibration of the FGGA with a single gas standard leads to additional uncertainty at mixing ratios largely different to the calibration value. Thus a multiple-point calibration scheme is required for enhanced accuracy.

3.3 Cross sensitivity to H_2O

In the following, the cross sensitivity to water vapour (H_2O) is investigated. H_2O has strong absorbing bands even in the near infrared operation wavelength of the FGGA (λ = 1651 nm), and mixing ratios in the atmosphere that can vary by three orders of magnitude between the ground (up to 30 000 ppm, 1 ppm = 1 µmol mol^{-1}) and the lower stratosphere (down to ∼ 3 ppm). Even if no direct spectroscopic interference would be present, molecules with large abundance can affect the spectral lineshape function of the target absorber by molecular collisions, which is being observed as a modified width of the lineshape function (Varghese and Hanson, 1984; Tuzson et al., 2010). The FGGA has a built-in humidity correction, and both wet and dry CH_4 data can be analysed. During initial testing of our FGGA model, we found that the built-in correction did not sufficiently account for large humidity changes. In particular, we found a residual sensitivity of around 3 ppb CH_4 at a humidity of 10 000 ppm. While this is already very good, for best possible accuracy we decided to quantify the cross sensitivity in the laboratory in order to apply a correction to the wet airborne CH_4 measurements.

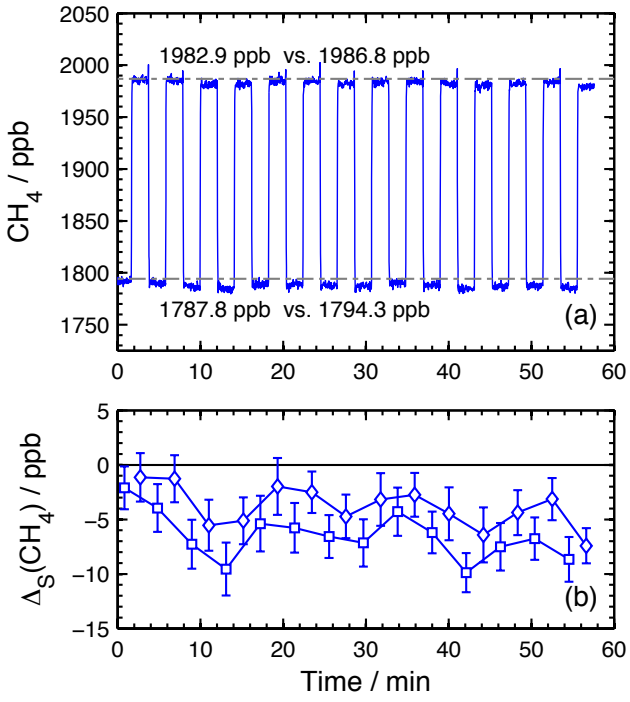

Fig. 4. (a) Sequential measurement of two known calibration gas mixtures (1986.8 ppb, 1794.3 ppb) yielded an accuracy within the 60 min measurement time of 6.5 ppb (< 0.5 %). Horizontal lines indicate the mixing ratio of the respective gas standard as determined by gas chromatography. **(b)** Difference of average FGGA measurements to gas standard mixing ratio (⋄ 1986.8 ppb; □ 1794.3 ppb). The accuracy is mostly determined by instrumental drift.

As performed in previous studies (Nara et al., 2012; Chen et al., 2013; Rella et al., 2013) we empirically determine a correction function by supplying a gas mixture of known CH_4 and varying H_2O mixing ratios, where the latter spans the humidity range experienced in flight.

A main flow of a dry calibration-gas standard is provided to the inlet of the instrument. Additionally, a small flow of the same gas is humidified in a gas bubbler, and it is subsequently diluted into the main flow. The flow rate of the small flow is adjusted to stepwise achieve a number of humidity levels between dry gas and around 15 000 ppm.

The humidity is measured with relatively low precision by the FGGA probing a weak H_2O absorption line in the vicinity of the CH_4 absorption line (Fig. 2). A dew-point hygrometer (Model DewMaster, EdgeTech, Marlborough, MA, USA) is operated in parallel and is used for humidity-calibration purposes.

In a first step of the analysis, the humidity measurements of the FGGA are calibrated using the dew-point hygrometer measurements by making use of a polynomial of second order (Fig. 5a). In the second step, the humidity dependence of the CH_4 measurements is quantified by a linear function, which is a sufficient approximation within the measurement uncertainty range (Fig. 5b).

The humidity-correction function was determined periodically in the laboratory. On average we found for this particular FGGA a correction function of

$$CH_4(\text{dry}) = CH_4(\text{moist}) - H_2O\ 2.3 \times 10^{-3}\ \frac{\text{ppb}\,(CH_4)}{\text{ppm}(H_2O)}. \quad (3)$$

The slope varied by ±10 %, which translates into an uncertainty of ±4.6 ppb (0.25 %) at $CH_4 = 1900$ ppb and a humidity of 10 000 ppm. Furthermore, the humidity measurements are associated with an uncertainty of ∼ 5 %, which translates in a 0.12 % uncertainty of the humidity corrected CH_4 data.

At the aircraft cruising altitude (∼ 220 hPa, > 10 000 m), where around 93 % of the total measurement are obtained, the humidity is generally below 50 ppm. In this case the cross-sensitivity can be neglected, as the total uncertainty is defined by noise (precision) and general instrument accuracy. However, measurements are also obtained during aircraft ascent and descent, which allows the derivation of vertical profiles above the respective airports. In this case the correction function effectively compensates for the humidity bias.

While the FGGA provides H_2O measurements itself, for the processing of our airborne data we use H_2O measurements obtained by a dedicated instrument (Brenninkmeijer et al., 2007), which offers far superior precision and accuracy. In that respect, the FGGA H_2O measurements serve as a redundant measurement in case the main H_2O measurements may not be available.

3.4 Calibration

Instrument calibration during airborne operation is a prerequisite to achieve the necessary accuracy for valid data interpretation. The best strategy would be an in-flight calibration with multiple (2–3) calibration gas mixtures. These standards would have to be provided aboard the aircraft, which is impractical in CARIBIC due to space restrictions. Calibration in the laboratory is usually performed before each flight. However, due to necessary ground-tests and instrument/container transportation, several days may pass between instrument calibration and actual flight series. Generally, the last flight of a series takes place at least 5–6 days after the instrument leaves our laboratory. We have therefore developed a calibration routine utilising CH_4 flask-sample measurements obtained simultaneously during all CARIBIC flights.

During each flight 14–45 air samples are obtained with two different sampler systems. (1) TRAC: 28 2.7 L glass flasks are filled with compressed ambient air and later analysed for greenhouse gases (GHGs), non-methane carbon hydrates (NMCHs), and halocarbons. (2) HIRES: 88 1 L stainless steel flasks are filled with compressed ambient air and later analysed for GHGs and NMCHs. The analyses are performed with high accuracy in various laboratories (Schuck et al., 2009; Baker et al., 2010; O'Sullivan, 2007; Batenburg et al., 2012).

For the calibration, the FGGA CH_4 measurements are first averaged over the effective sampling times (0.5–4 min) during which the air samples were obtained. The CH_4 mixing ratios of each individual sample are then used to derive a piecewise linear calibration function for the FGGA CH_4 data between two consecutive flask samples. For FGGA measurements before the first and after the last air sample, the calibration is linearly extrapolated based on the first and last two air samples, respectively.

Figure 6a shows as an example the CH_4 measurements of the flask samples and the respective FGGA data on a flight from Bogota to Frankfurt departing on 23 March 2011. Note that for this figure the FGGA in situ CH_4 data are corrected for slope and offset by an average calibration function of this particular flight (black dashed line), which has for this particular flight a slope of 0.9971 and an ordinate (bias) of 26.46 ppb. This depiction better illustrates the scattering of the CH_4 measurements with respect to the calibration function. It is also later being used for further data-quality analyses.

The FGGA was calibrated before the four flights in March 2011 in the laboratory. We attribute the relatively large offset to the fact that usually about one week passes between calibration and actual flight, including several instrument starts as part of ground tests. During the flight sequences we generally observed a flight-to-flight variability of the offset of 5–10 ppb, which occasionally reached 15 ppb. This changing offset further emphasises on the need for instrument calibration based on measurements taken during flight. Note that we do not consider zero-gas measurements, because the natural CH_4 variability (range) during every one flight generally provides a well enough defined calibration function.

Figure 6b shows the raw CH_4 measurements (grey trace), the CH_4 measurements obtained from the flask samples (red crosses), as well as the calibrated in situ CH_4 measurements along the flight (blue trace). The altitude profile is also depicted (black trace).

4 Airborne uncertainty assessment

During unattended instrument deployment aboard aircraft, rather large changes in environmental conditions occur. For instance, the cabin pressure aboard the CARIBIC aircraft varies from 1000 hPa on the ground to around 815 hPa at cruising altitude, which may lead to subtle changes in the optical alignment of, for example, the ICOS cavity. Furthermore, the temperature in the container can be as low as 15 °C

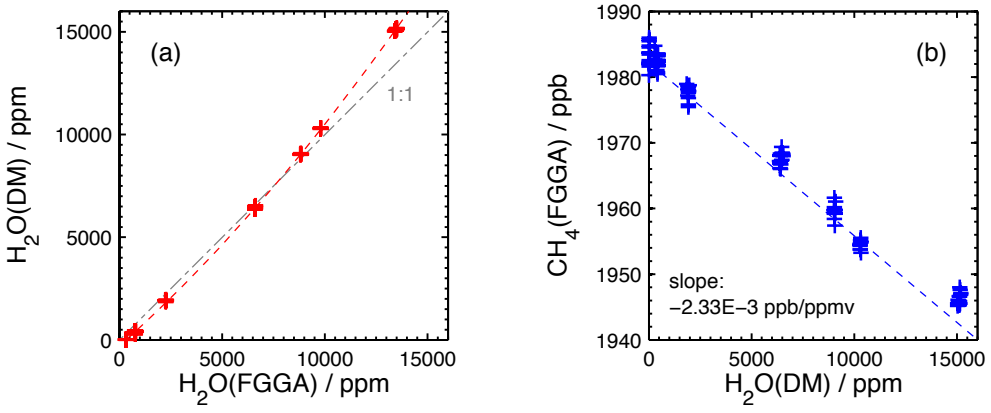

Fig. 5. (a) Calibration polynomial (dashed line) of the FGGA H_2O measurements. **(b)** Humidity dependence of the CH_4 measurements approximated by a linear correction function (dashed line). Note that measurements are evaluated and presented as 30 s averages.

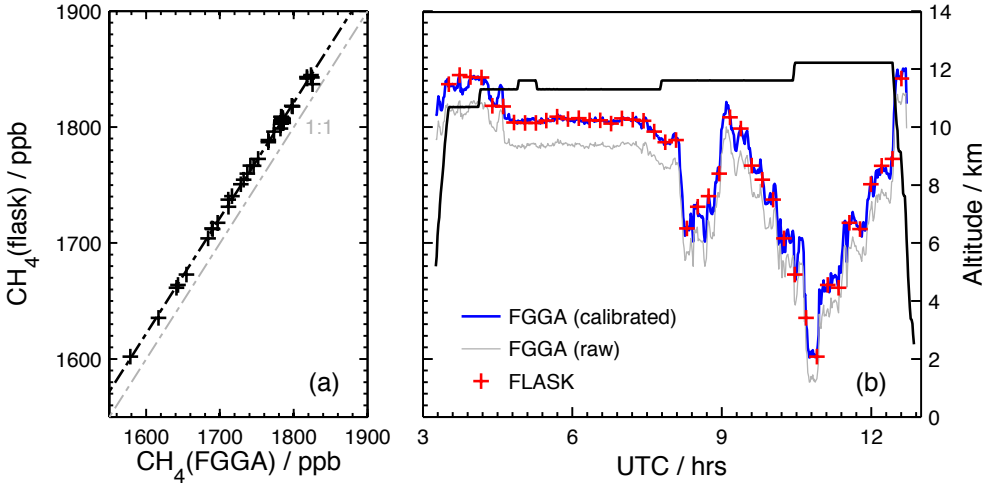

Fig. 6. (a) Depiction of the linear calibration function derived for flight LH336 from Bogota to Frankfurt departing on 23 March 2011. For this flight we find a mean calibration function with a slope 0.9971 and ordinate of 26.46 ppb. **(b)** Calibrated FGGA CH_4 measurements (solid blue trace, 10 s averages) and simultaneously obtained flask sample measurements (red +) on flight LH336. The grey trace depicts the uncalibrated FGGA measurements. The black trace shows the altitude profile for this flight.

and, in extreme cases, rises up to 40 °C. It is thus important to note that the instrument performance may suffer under airborne conditions.

Therefore, we have performed a detailed uncertainty assessment under airborne conditions based on a statistical analysis of all FGGA flight data. The 103 flights were performed between October 2010 and July 2013. During this time 2780 CH_4 measurements were obtained from the simultaneously collected flask samples.

4.1 Replication precision

In the laboratory, we have analysed the instrument precision by means of the Allan variance method. During airborne operation, this technique is not applicable due to additional, usually dominating atmospheric variability of CH_4. We have thus investigated the short term precision of in-flight measurements by calculating the standard deviation of 10 s averages. Figure 7 shows the corresponding probability density function (PDF) of the calculated standard deviations.

It is found that, on average, the airborne 1-σ precision of the instrument for 10 s data averaging is 2 ppb. This is in good agreement (factor of two) with the Allan variance depicted in Fig. 3. About 90 % of our measurements show a precision of better than 4.5 ppb. Note however, that natural variability is likely to increase the standard deviation, even on a 10 s time scale. This manifests itself in the somewhat wider tail of the PDF towards higher $\sigma(CH_4)$.

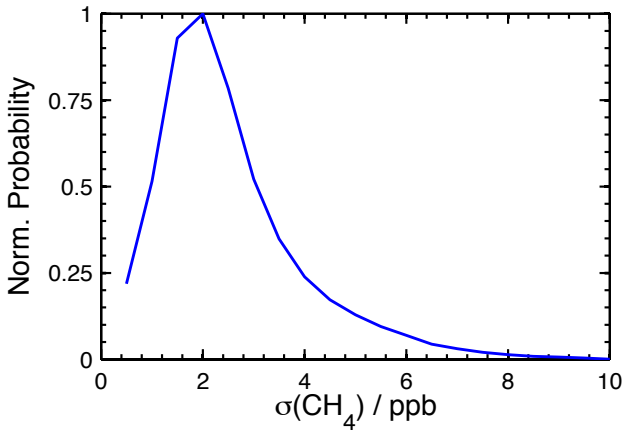

Fig. 7. PDF of the standard deviation of CH_4 measurements obtained airborne (10 s averages). The precision during our airborne measurements is better than 2 ppb for more than 50 % of the time, and better than 4.5 ppb for more than 90 % of the time.

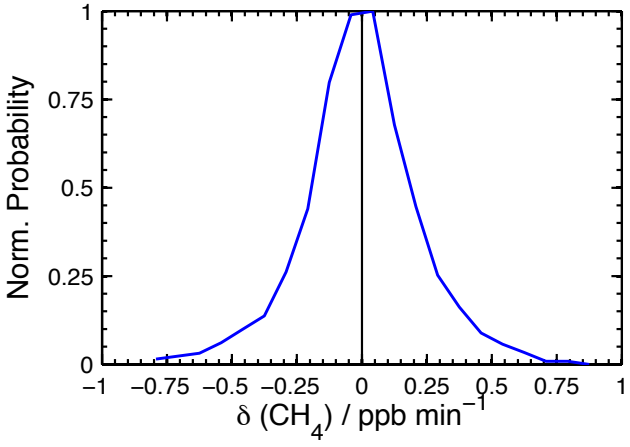

Fig. 8. PDF of the instrumental drift during airborne operation inferred from calibration to CH_4 flask-sample measurements. The standard deviation (1σ) is 0.24 ppb min^{-1}.

4.2 Drift analysis

A statistical analysis of instrumental drift in flight conditions was performed. First the difference $d(CH_4)$ between FGGA and flask is calculated for every coincident calibration measurement n

$$d(CH_4)_n = CH_4(FGGA)_n - CH_4(flask)_n. \quad (4)$$

The instrumental drift $\delta(CH_4)$ is approximated as the difference in the deviation $d(CH_4)$ of consecutive measurements normalised by the elapsed time t

$$\delta(CH_4)_i = \frac{d(CH_4)_n - d(CH_4)_{n-1}}{t_n - t_{n-1}}. \quad (5)$$

We note that this method assumes linear drift during the time interval $[t_{n-1}\ t_n]$. This may not always be valid during flight, but is the only method applicable given the limited number of flask samples.

The observed deviation between FGGA and flask from one calibration measurement to the next is partly determined by the relative uncertainty (precision) of the measurements. However, it is mostly defined by instrumental drift between calibration measurements (15–45 min), which is longer than the stability time of the instrument (80 s in the laboratory).

Figure 8 shows the corresponding PDF of δCH_4 for all CARIBIC flights considered here. The average drift is zero, and the PDF is symmetric, which indicates a random effect. An instrumental drift of about 0.24 ppb min^{-1} (1σ) is derived from the PDF.

To bring this finding into perspective, we can compare δCH_4 with the results obtained by the Allan-variance analysis. $\delta CH_4 = 0.24$ ppb min^{-1} suggests that the instrument will have drifted by 2.4 ppb after 600 s assuming linear drift. Comparing to the Allan plot (Fig. 3), we deduce in the laboratory a drift of ~ 1.2 ppb after the same time. This suggests, that under airborne conditions, the instrumental drift is $\sim 2\times$ larger than in the laboratory.

There are some occasions where the instrument was not yet properly warmed up when we started the measurement in flight. Then we sometimes observed what might be a direct correlation of temperature and $d(CH_4)$. However, it is difficult to fully disentangle the processes that lead to changes in $d(CH_4)$. At the cruising altitude, where most measurements are taken, the cabin pressure is rather constant, and we may rule out any pressure-induced drift.

The average time between flask samples during all CARIBIC flights considered here was $\sim 16 \pm 5$ min, during which the instrument may have drifted by 4 ± 1.25 ppb. The samples are collected according to a pre-determined time schedule and therefore variations in the flight schedule cannot be compensated. Generally no air samples are obtained during aircraft descent. The average measurement time before a flask sample was obtained after aircraft take off was 16.5 ± 3 min. During aircraft descent, measurements were taken for 47 ± 18 min after the last flask sample was obtained. Again assuming linear drift we estimate the uncertainty of our CH_4 measurements at the beginning and the end of a flight to be 4.2 ± 0.75 ppb and 11.75 ± 4.5 ppb, respectively.

4.3 Accuracy

For the analysis of the instrument accuracy it is not possible to directly compare the flask-sample measurements and the corresponding corrected FGGA measurements. By definition these measurements are identical to the flask measurements after applying the calibration procedure described in Sect. 3.4. We have therefore used a slightly different approach to estimate the instrument accuracy.

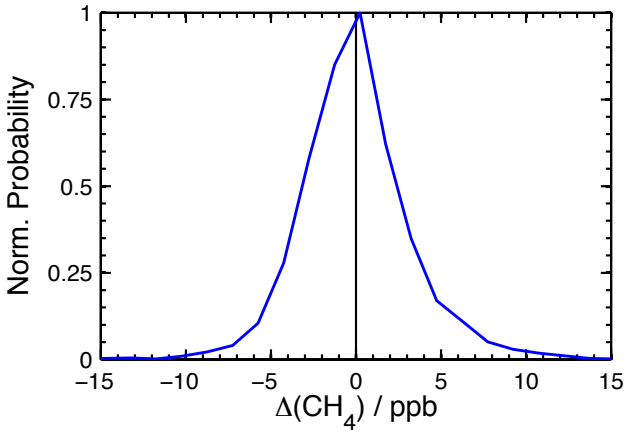

Fig. 9. PDF of the airborne accuracy expressed as deviation of the individual airborne calibration measurements from the linear calibration function for each flight. On average the accuracy is found to be $\Delta CH_4 \sim 3.4$ ppb (1σ) at the aircraft cruising altitude.

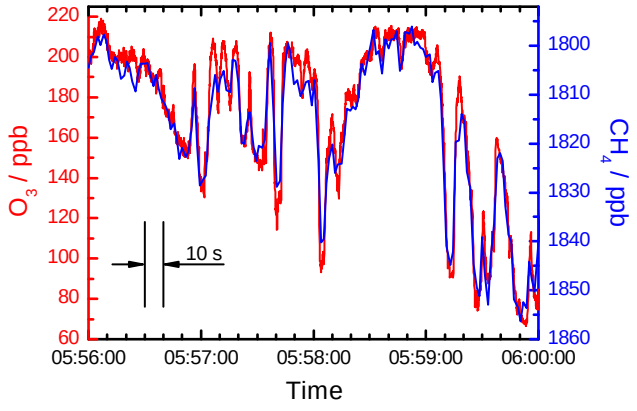

Fig. 10. Small-scale filamentary structures of CH_4 (blue, 1 Hz) and O_3 (red, 5 Hz) observed during a time period of 4 min (60 km flight distance) around the tropopause during a flight from Caracas to Frankfurt on 18 September 2013. Note the inverted scale of CH_4.

First we calculate a single linear calibration function

$$CH_4(\mathrm{FGGA})^* = a_i CH_4(\mathrm{FGGA}) + b_i, \quad (6)$$

for every flight i (Fig. 6a). This function is then applied to the FGGA measurements. The average slope of the calibration function is 0.947 ± 0.122 for all 103 flights.

The accuracy of our measurements $\Delta(CH_4)$ is then expressed as the deviation of the linearly corrected individual FGGA measurements to their respective flask sample measurements

$$\Delta(CH_4)_n = [a_i CH_4(\mathrm{FGGA})_n + b_i] - CH_4(\mathrm{flask})_n. \quad (7)$$

The PDF of $\Delta(CH_4)$ of all 2780 calibration measurements is shown in Fig. 9. On average (103 flights) we obtain a distribution that reveals an uncertainty of ~ 3.4 ppb (1σ) at the aircraft cruising altitude where flask samples are obtained.

We note that this method of obtaining an accuracy estimate most likely overestimates the measurement uncertainty, since using a piece-wise calibration function for the reported flight data reduces deviations by linear interpolation between flask measurements.

4.4 Total uncertainty

The total uncertainty of the CH_4 measurements is determined by the relative uncertainty (precision, $\sigma(CH_4)$), and the uncertainty of the absolute value (accuracy, $\Delta(CH_4)$). The former is dependent on the averaging time. We report in-situ data as 10 s averages, where the precision was determined to be $\sigma(CH_4) = 2$ ppb. The accuracy at flight level was determined to be $\Delta(CH_4) = 3.4$ ppb, which includes the relative uncertainty and instrumental drift terms. During ascent and descent of the aircraft, no flask samples are obtained. Depending on the time to the closest calibration event, instrumental drift is estimated to reduce the accuracy by up to 11.75 ppb during the aircraft descent, i.e. 47 min after the last flask sample was obtained. Furthermore, the analysis of the flask samples is stated with an uncertainty of 1.8 ppb (Schuck et al., 2009).

From the individual uncertainties we can derive the total uncertainty of our in situ CH_4 measurements as the sum of the individual uncertainty terms. At flight level we achieve measurements with an uncertainty of 3.85 ppb (0.2 % for an average $CH_4 \sim 1800$ ppb). During aircraft ascent and descent, where instrumental drift becomes more relevant, we estimate the uncertainty to be 12.4 ppb (0.7 %) for measurements obtained at the lowest sampling altitude of 2 km.

4.5 Response time

The temporal resolution of the FGGA is inferred by comparing fast fluctuations in CH_4 with data recorded by the fast chemiluminescence ozone detector described in Zahn et al. (2012). At the tropopause and lowermost stratosphere (LMS) both species are highly anticorrelated as ozone increases but methane decreases with height above the mid-latitude tropopause (see Sect. 5.2).

Figure 10 shows a short-time cross-section of CH_4 and O_3 observed just above the chemical tropopause of $O_3 \sim 75$ ppbv (see Zahn and Brenninkmeijer, 2003; Thouret et al., 2006) on a flight from Caracas to Frankfurt. The 5 Hz ozone data indicate fast fluctuations in the 0.5–10 s range, most likely generated by gravity waves. The CH_4 data (blue) is recorded with 1 Hz, i.e. each point indicates 1 s or 250 m along the flight path. The compact anticorrelation of both species is nicely visible and little smoothing of the CH_4 data is resolved. Indeed, the volume sample flow of ~ 22 vol-L min^{-1} (see Sect. 2) together with the volume of the cavity of ~ 0.5 L suggests a time resolution of 1.4 s.

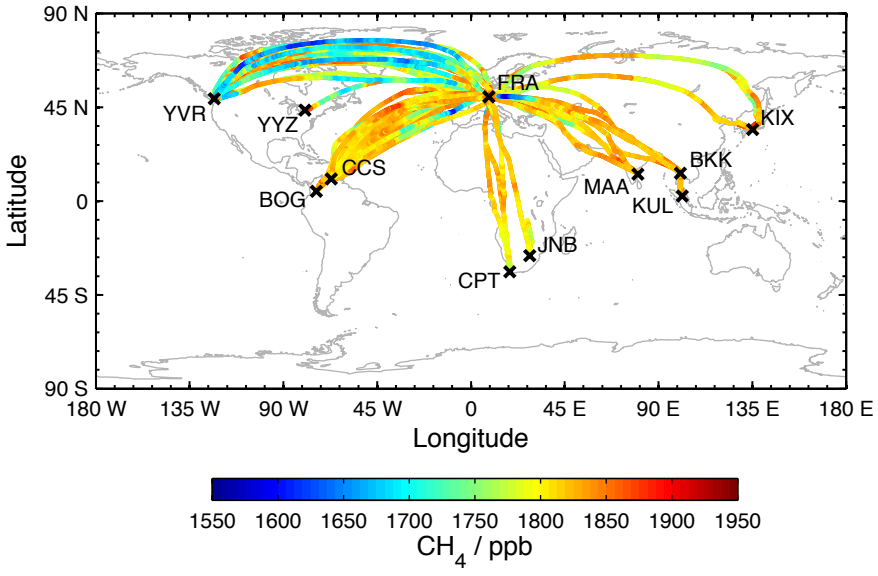

Fig. 11. Map of 103 measurement flights originating from Frankfurt, Germany (FRA) that have been performed during the first 2.5 yr of instrument operation. Data are averaged for 60 s. The colour code represents the CH_4 mixing ratio. Destinations are FRA: Frankfurt, BKK: Bangkok, BOG: Bogota, CCS: Caracas, CPT: Cape Town, JNB: Johannesburg, KIX: Osaka, KUL: Kuala Lumpur, MAA: Chennai, YYZ: Toronto, YVR: Vancouver.

5 Airborne operation

5.1 Near-global CH_4 measurements

The instrument described in the present paper has been deployed for four consecutive long-distance flights per month aboard the CARIBIC passenger aircraft since October 2010. Flights originate from Frankfurt, Germany (50° N, 8° E) to various destinations worldwide (Fig. 11). In total, CH_4 was measured in situ during 103 flights between October 2010 and July 2013. The flights took place mostly in the northern hemispheric upper troposphere and lowermost stratosphere (UT/LMS), and occasionally lead across the tropics to southern Africa. Note that the available flight destinations of the CARIBIC aircraft are determined by the semi-annual Lufthansa flight schedule for this particular aircraft, which limits the number of possible flight routes. The instrument operation will continue until at least 2014.

The CH_4 measurements are calibrated using the flask sample data as described in Sect. 3.4. The cross sensitivity of the CH_4 measurements to H_2O is corrected by a linear correction function employing the humidity measurements also measured in the CARIBIC container.

Figure 11 shows the measurements obtained during the first 2.5 yr of operation along flight routes between Frankfurt (Germany) to ten destinations in North/South America, South Africa, and Asia. The colour code represents the CH_4 mixing ratio (60 s averages).

Methane is a medium-lived greenhouse gas with an atmospheric lifetime of ∼ 9 yr (Dlugokencky et al., 2011) and thus shows modest variations by up to ∼ 20 % in the upper troposphere (UT), as seen in Fig. 11. These variations are mainly due to the differing origin and nature of the air masses encountered in the UT.

Presently, the globally averaged CH_4 mixing ratio is around 1800 ppb (Dlugokencky et al., 2011). The elevated CH_4 mixing ratios of up to 1950 ppb are indicative of polluted air masses and are thus often encountered downwind of the continents, e.g. imbedded in warm conveyor belt systems starting, for example, in the gulf of Mexico and reaching the upper troposphere over the mid-Atlantic (Eckhardt et al., 2004). The weak seasonal variation of CH_4 of ∼ 30 ppb in the mid-latitude UT (not shown) is not resolved in Fig. 11 and leads to some further variability.

The most drastic feature in Fig. 11 is the detection of stratospheric air north of ∼ 35° N where the CH_4 mixing ratio drops down to 1600 ppb in spring when CH_4-poor air descends from the higher stratosphere within the downward branch of the Brewer Dobson circulation.

Note the sometimes very sharp gradients in the CH_4 mixing ratio, especially when crossing the local tropopause, which cannot be captured by the flask samples taken on average each 225 km at cruising altitude.

5.2 Tracer-tracer correlation

One powerful test to assess the uncertainty of the CH_4 data during a flight is the correlation with another tracer that can very accurately be measured and that is controlled by the same atmospheric process. In CARIBIC, ozone (O_3) is measured with a total uncertainty of 1–2 % (an uncertainty

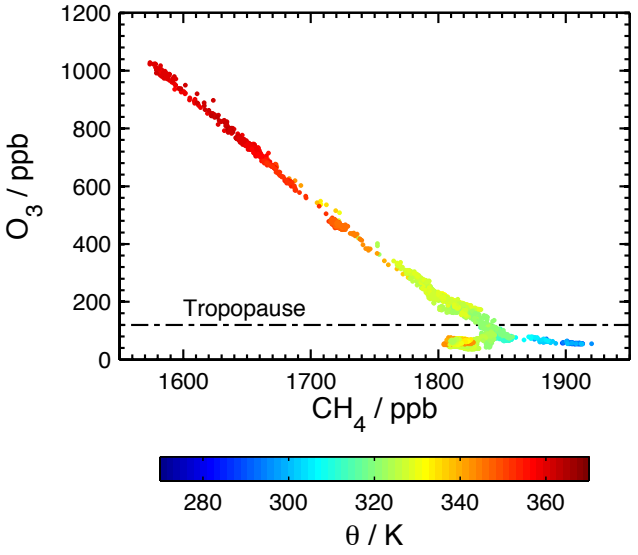

Fig. 12. CH_4–O_3 correlation on a flight from Bangkok to Frankfurt on 21 March 2013 (colour code: potential temperature θ).

that is mainly determined by the uncertainty in spectroscopic data), but with a reproducibility of better than 0.5 %. In spring when O_3-rich and CH_4-poor high stratospheric air descends in mid- and high-latitudes, both O_3 and CH_4 constitute very long-lived (basically inert) transport tracers in the lower stratosphere and are virtually unaffected by variations in the troposphere. And indeed, as shown in Fig. 12, O_3 and CH_4 are compactly correlated above the tropopause (above $O_3 \sim 120$ ppb) during this flight. There is a weak influence due to the mixing with upper tropospheric air within the first 1.0–1.5 km above the tropopause (up to $O_3 = 300$ ppb). Above this level and up to 5 km above the tropopause ($O_3 = 1000$ ppb) the correlation is very tight. These stratospheric data have been recorded over a time of ~ 4.5 h or ~ 3500 km.

6 Conclusions

The setup, characterisation, and airborne deployment of a laser spectrometer to measure CH_4 mixing ratios in situ aboard a passenger aircraft have been described. The airborne instrument is based on a commercial fast methane analyser (FGGA, Los Gatos Research), which has been largely modified to meet aircraft requirements and to be operated autonomously.

Laboratory characterisation by means of the Allan variance method has revealed a precision of ~ 0.96 ppb and 0.6 ppb for an averaging time of 10 s and 80 s, respectively. The CH_4 data can be averaged for as long as 80 s after which instrumental drift starts to become relevant, and the precision is not further improved. The in-flight precision is found to be 2 ppb (1σ), which is in agreement with the laboratory results within a factor of 2.

Using the standard single-point calibration suggested for the FGGA, an uncertainty of ~ 6.5 ppb has been determined in the laboratory using known calibration gas standards. Besides instrumental drift, the instrument accuracy is affected by a cross-sensitivity of the CH_4 measurements to the H_2O mixing ratio. This cross sensitivity has been quantified in the laboratory to be around 4.6 ppb when the humidity reaches lower tropospheric mixing ratios (10 000 ppm). A linear correction function is applied to reduce this humidity bias.

As a means to calibrate the in situ CH_4 measurements, a calibration method has been developed that utilises CH_4 measurements from flask samples obtained during the same flights. Furthermore, we make use of in situ H_2O measurements in order to apply a humidity-bias correction. With this calibration method we achieved a total uncertainty of 3.85 ppb (1σ) for measurements obtained at the aircraft cruising altitude. During ascent and descent of the aircraft, where no flask samples are obtained, instrumental drift affects the measurements stronger. Then the total uncertainty at lower altitudes (~ 2 km) is estimated to be ~ 12.4 ppb (1σ).

Airborne measurements in a large part of the northern hemispheric UT/LMS, and to some extend in the Southern Hemisphere, were obtained during the first two and a half years of monthly operation. The data quality and the spatial resolution are well sufficient to study e.g. small-scale air mass transport across the tropopause.

Acknowledgements. We thank D. Scharffe, C. Köppel, and S. Weber for handling the CARIBIC instrumentation prior and after flights. We acknowledge support by Deutsche Forschungsgemeinschaft and Open Access Publishing Fund of Karlsruhe Institute of Technology.

The service charges for this open access publication have been covered by a Research Centre of the Helmholtz Association.

Edited by: W. R. Simpson

References

Baer, D. S., Paul, J. B., Gupta, M., and O'Keefe, A.: Sensitive absorption measurements in the near-infrared region using off-axis integrated-cavity-output spectroscopy, Appl. Phys. B, 75, 261–265, doi:10.1007/s00340-002-0971-z, 2002.

Baker, A. K., Slemr, F., and Brenninkmeijer, C. A. M.: Analysis of non-methane hydrocarbons in air samples collected aboard the CARIBIC passenger aircraft, Atmos. Meas. Tech., 3, 311–321, doi:10.5194/amt-3-311-2010, 2010.

Batenburg, A. M., Schuck, T. J., Baker, A. K., Zahn, A., Brenninkmeijer, C. A. M., and Röckmann, T.: The stable isotopic composition of molecular hydrogen in the tropopause region probed by the CARIBIC aircraft, Atmos. Chem. Phys., 12, 4633–4646, doi:10.5194/acp-12-4633-2012, 2012.

Berman, E. S. F., Fladeland, M., Liem, J., Kolyer, R., and Gupta, M.: Greenhouse gas analyser for measurements of

carbon dioxide, methane, and water vapor aboard an unmanned aerial vehicle, Sensor Actuat B-Chem., 169, 128–135, doi:10.1016/j.snb.2012.04.036, 2012.

Bloom, A. A., Palmer, P. I., Fraser, A., Reay, D. S., and Frankenberg, C.: Large-Scale Controls of Methanogenesis Inferred from Methane and Gravity Spaceborne Data, Science, 327, 322–325, doi:10.1126/science.1175176, 2010.

Brenninkmeijer, C. A. M., Crutzen, P., Boumard, F., Dauer, T., Dix, B., Ebinghaus, R., Filippi, D., Fischer, H., Franke, H., Frieß, U., Heintzenberg, J., Helleis, F., Hermann, M., Kock, H. H., Koeppel, C., Lelieveld, J., Leuenberger, M., Martinsson, B. G., Miemczyk, S., Moret, H. P., Nguyen, H. N., Nyfeler, P., Oram, D., O'Sullivan, D., Penkett, S., Platt, U., Pupek, M., Ramonet, M., Randa, B., Reichelt, M., Rhee, T. S., Rohwer, J., Rosenfeld, K., Scharffe, D., Schlager, H., Schumann, U., Slemr, F., Sprung, D., Stock, P., Thaler, R., Valentino, F., van Velthoven, P., Waibel, A., Wandel, A., Waschitschek, K., Wiedensohler, A., Xueref-Remy, I., Zahn, A., Zech, U., and Ziereis, H.: Civil Aircraft for the regular investigation of the atmosphere based on an instrumented container: The new CARIBIC system, Atmos. Chem. Phys., 7, 4953–4976, doi:10.5194/acp-7-4953-2007, 2007.

Chen, H., Winderlich, J., Gerbig, C., Hoefer, A., Rella, C. W., Crosson, E. R., Van Pelt, A. D., Steinbach, J., Kolle, O., Beck, V., Daube, B. C., Gottlieb, E. W., Chow, V. Y., Santoni, G. W., and Wofsy, S. C.: High-accuracy continuous airborne measurements of greenhouse gases (CO_2 and CH_4) using the cavity ring-down spectroscopy (CRDS) technique, Atmos. Meas. Tech., 3, 375–386, doi:10.5194/amt-3-375-2010, 2010.

Chen, H., Karion, A., Rella, C. W., Winderlich, J., Gerbig, C., Filges, A., Newberger, T., Sweeney, C., and Tans, P. P.: Accurate measurements of carbon monoxide in humid air using the cavity ring-down spectroscopy (CRDS) technique, Atmos. Meas. Tech., 6, 1031–1040, doi:10.5194/amt-6-1031-2013, 2013.

Collins, J. E., Sachse, G. W., Anderson, B. E., Weinheimer, A. J., Walega, J. G., and Ridley, B. A.: AASE-II in-situ tracer correlations of methane, nitrous oxide, and ozone as observed aboard the DC-8, Geophys. Res. Lett., 20, 2543–2546, doi:10.1029/93GL02624, 1993.

Crosson, E. R.: A cavity ring-down analyser for measuring atmospheric levels of methane, carbon dioxide, and water vapor, Appl. Phys. B, 92, 403–408, doi:10.1007/s00340-008-3135-y, 2008.

Dlugokencky, E. J., Myers, R. C., Lang, P. M., Masarie, K. A., Crotwell, A. M., Thoning, K. W., Hall, B. D., Elkins, J. W., and Steele, L. P.: Conversion of NOAA atmospheric dry air CH_4 mole fractions to a gravimetrically prepared standard scale, J. Geophys. Res., 110, D18306, doi:10.1029/2005JD006035, 2005.

Dlugokencky, E. J., Bruhwiler, L., White, J. W. C., Emmons, L. K., Novelli, P. C., Montzka, S. A., Masarie, K. A., Lang, P. M., Crotwell, A. M., Miller, J. B., and Gatti, L. V.: Observational constraints on recent increases in the atmospheric CH_4 burden, Geophys. Res. Lett., 36, L18803, doi:10.1029/2009GL039780, 2009.

Dlugokencky, E. J., Nisbet, E. G., Fisher, R., and Lowry, D.: Global atmospheric methane: budget, changes and dangers, Philos. T. Roy. Soc. A, 369, 2058–2072, doi:10.1098/rsta.2010.0341, 2011.

Durry, G., Hauchecorne, A., Ovarlez, J., Ovarlez, H., Pouchet, I., Zeninari, V., and Parvitte, B.: In situ measurements of H_2O and CH_4 with telecommunication laser diodes in the lower stratosphere: dehydration and indication of a tropical air instrusion at mid-latitudes, J. Atmos. Chem., 43, 175–194, 2002.

Dyroff, C.: Optimum signal-to-noise ratio in off-axis integrated cavity output spectroscopy, Opt. Lett., 36, 1110–1112, doi:10.1364/OL.36.001110, 2011.

Eckhardt, S., Stohl, A., Wernli, H., James, P., Forster, C., and Spichtinger, N.: A 15-Year Climatology of Warm Conveyor Belts, J. Climate, 17, 218–237, doi:10.1175/1520-0442(2004)017<0218:AYCOWC>2.0.CO;2, 2004.

Gurlit, W., Zimmermann, R., Giesemann, C., Fernholz, T., Ebert, V., Wolfrum, J., Platt, U., and Burrows, J. P.: Lightweight diode laser spectrometer CHILD (Compact High-altitude In-situ Laser Diode) for balloonborne measurements of water vapor and methane, Appl. Optics, 44, 91–102, 2005.

Heimann, M.: How Stable Is the Methane Cycle?, Science, 327, 1211–1212, doi:10.1126/science.1187270, 2010.

Heimann, M.: Enigma of recent methane budget, Nature, 476, 157–158, 2011.

Machida, T., Matsueda, H., Sawa, Y., Nakagawa, Y., Hirotani, K., Kondo, N., Goto, K., Nakazawa, T., Ishikawa, K., and Ogawa, T.: Worldwide Measurements of Atmospheric CO_2 and Other Trace Gas Species Using Commercial Airlines, J. Atmos. Ocean. Tech., 25, 1744–1754, doi:10.1175/2008JTECHA1082.1, 2008.

Nara, H., Tanimoto, H., Tohjima, Y., Mukai, H., Nojiri, Y., Katsumata, K., and Rella, C. W.: Effect of air composition (N_2, O_2, Ar, and H_2O) on CO_2 and CH_4 measurement by wavelength-scanned cavity ring-down spectroscopy: calibration and measurement strategy, Atmos. Meas. Tech., 5, 2689–2701, doi:10.5194/amt-5-2689-2012, 2012.

Nelson, D. D., McManus, B., Urbanski, S., Herndorn, S., and Zahniser, M. S.: High precision measurements of atmospheric nitrous oxide and methane using thermoelectrically cooled mid-infrared quantum cascade lasers and detectors, Spectrochim. Acta, Part A, 60, 3325–3335, 2004.

O'Connor, F. M., Boucher, O., Gedney, N., Jones, C. D., Folberth, G. A., Coppell, R., Friedlingstein, P., Collins, W. J., Chappellaz, J., Ridley, J., and Johnson, C. E.: Possible role of wetlands, permafrost, and methane hydrates in the methane cycle under future climate change: A review, Rev. Geophys., 48, RG000326, doi:10.1029/2010RG000326, 2010.

O'Shea, S. J., Bauguitte, S. J.-B., Gallagher, M. W., Lowry, D., and Percival, C. J.: Development of a cavity-enhanced absorption spectrometer for airborne measurements of CH4 and CO_2, Atmos. Meas. Tech., 6, 1095–1109, doi:10.5194/amt-6-1095-2013, 2013.

O'Sullivan, D. A.: Temporal and spatial variability of halogenated compounds and other trace gases, Ph.D. thesis, University of East Anglia, Norwich, United Kingdom, 2007.

Payan, S., Camy-Peyret, C., Oelhaf, H., Wetzel, G., Maucher, G., Keim, C., Pirre, M., Huret, N., Engel, A., Volk, M. C., Kuellmann, H., Kuttippurath, J., Cortesi, U., Bianchini, G., Mencaraglia, F., Raspollini, P., Redaelli, G., Vigouroux, C., De Mazière, M., Mikuteit, S., Blumenstock, T., Velazco, V., Notholt, J., Mahieu, E., Duchatelet, P., Smale, D., Wood, S., Jones, N., Piccolo, C., Payne, V., Bracher, A., Glatthor, N., Stiller, G., Grunow, K., Jeseck, P., Te, Y., and Butz, A.: Validation of version-4.61 methane and nitrous oxide observed by MIPAS, Atmos. Chem. Phys., 9, 413–442, doi:10.5194/acp-9-413-2009, 2009.

Rella, C. W., Chen, H., Andrews, A. E., Filges, A., Gerbig, C., Hatakka, J., Karion, A., Miles, N. L., Richardson, S. J., Steinbacher, M., Sweeney, C., Wastine, B., and Zellweger, C.: High accuracy measurements of dry mole fractions of carbon dioxide and methane in humid air, Atmos. Meas. Tech., 6, 837–860, doi:10.5194/amt-6-837-2013, 2013.

Richard, E. C., Kelly, K. K., Winkler, R. H., Wilson, R., Thompson, T. L., McLaughlin, R. J., Schmeltekopf, A. L., and Tuck, A. F.: A fast-response near-infrared tunable diode laser absorption spectrometer for in situ measurements of CH_4 in the upper troposphere and lower stratosphere, Appl. Phys. B, 75, 183–194, 2002.

Riese, M., Ploeger, F., Rap, A., Vogel, B., Konopka, P., Dameris, M., and Forster, P.: Impact of uncertainties in atmospheric mixing on simulated UTLS composition and related radiative effects, J. Geophys. Res., 117, D16305, doi:10.1029/2012JD017751, 2012.

Rothman, L., Gordon, I., Barbe, A., Benner, D., Bernath, P., Birk, M., Boudon, V., Brown, L., Campargue, A., Champion, J.-P., Chance, K., Coudert, L., Dana, V., Devi, V., Fally, S., Flaud, J.-M., Gamache, R., Goldman, A., Jacquemart, D., Kleiner, I., Lacome, N., Lafferty, W., Mandin, J.-Y., Massie, S., Mikhailenko, S., Miller, C., Moazzen-Ahmadi, N., Naumenko, O., Nikitin, A., Orphal, J., Perevalov, V., Perrin, A., Predoi-Cross, A., Rinsland, C., Rotger, M., Simecková, M., Smith, M., Sung, K., Tashkun, S., Tennyson, J., Toth, R., Vandaele, A., and Auwera, J. V.: The HITRAN 2008 molecular spectroscopic database, J. Quant. Spectrosc. Ra., 110, 533–572, doi:10.1016/j.jqsrt.2009.02.013, 2009.

Sayres, D. S., Moyer, E. J., Hanisco, T. F., Clair, J. M. S., Keutsch, F. N., O'Brien, A., Allen, N. T., Lapson, L., Demusz, J. N., Rivero, M., Martin, T., Greenberg, M., Tuozzolo, C., Engel, G. S., Kroll, J. H., Paul, J. B., and Anderson, J. G.: A new cavity based absorption instrument for detection of water isotopologues in the upper troposphere and lower stratosphere, Rev. Sci. Instrum., 80, 044102, doi:10.1063/1.3117349, 2009.

Schneising, O., Buchwitz, M., Burrows, J. P., Bovensmann, H., Bergamaschi, P., and Peters, W.: Three years of greenhouse gas column-averaged dry air mole fractions retrieved from satellite – Part 2: Methane, Atmos. Chem. Phys., 9, 443–465, doi:10.5194/acp-9-443-2009, 2009.

Schuck, T. J., Brenninkmeijer, C. A. M., Slemr, F., Xueref-Remy, I., and Zahn, A.: Greenhouse gas analysis of air samples collected onboard the CARIBIC passenger aircraft, Atmos. Meas. Tech., 2, 449–464, doi:10.5194/amt-2-449-2009, 2009.

Schuck, T. J., Ishijima, K., Patra, P. K., Baker, A. K., Machida, T., Matsueda, H., Sawa, Y., Umezawa, T., Brenninkmeijer, C. A. M., and Lelieveld, J.: Distribution of methane in the tropical upper troposphere measured by CARIBIC and CONTRAIL aircraft, J. Geophys. Res., 117, D19304, doi:10.1029/2012JD018199, 2012.

Scott, D. C., Herman, R. L., Webster, C. R., May, R. D., Flesch, G. J., and Moyer, E. J.: Airborne Laser Infrared Absorption Spectrometer (ALIAS-II) for In Situ Atmospheric Measurements of N_2O, CH_4, CO, HCl, and NO_2 from Balloon or Remotely Piloted Aircraft Platforms, Appl. Optics, 38, 4609–4622, doi:10.1364/AO.38.004609, 1999.

Solomon, S., Qin, D., Manning, M., Chen, Z., Marquis, M., Averyt, K., Tignor, M., and Miller, H. (Eds.): Climate Change 2007: The Physical Science Basis. Contribution of Working Group I to the Fourth Assessment Report of the Intergovernmental Panel on Climate Change, Cambridge University Press, Cambridge, United Kingdom and New York, NY, USA, 2007.

Spackman, J. R., Weinstock, E. M., Anderson, J. G., Hurst, D. F., Jost, H. J., and Schauffler, S. M.: Aircraft observations of rapid meridional transport from the tropical tropopause layer into the lowermost stratosphere: Implications for midlatitude ozone, J. Geophys. Res., 112, D12308, doi:10.1029/2006JD007618, 2007.

Thouret, V., Cammas, J.-P., Sauvage, B., Athier, G., Zbinden, R., Nédélec, P., Simon, P., and Karcher, F.: Tropopause referenced ozone climatology and inter-annual variability (1994–2003) from the MOZAIC programme, Atmos. Chem. Phys., 6, 1033–1051, doi:10.5194/acp-6-1033-2006, 2006.

Tuzson, B., Hiller, R. V., Zeyer, K., Eugster, W., Neftel, A., Ammann, C., and Emmenegger, L.: Field intercomparison of two optical analysers for CH_4 eddy covariance flux measurements, Atmos. Meas. Tech., 3, 1519–1531, doi:10.5194/amt-3-1519-2010, 2010.

Varghese, P. L. and Hanson, R. K.: Collisional narrowing effects on spectral line shapes measured at high resolution, Appl. Optics, 23, 2376–2385, doi:10.1364/AO.23.002376, 1984.

Wecht, K. J., Jacob, D. J., Wofsy, S. C., Kort, E. A., Worden, J. R., Kulawik, S. S., Henze, D. K., Kopacz, M., and Payne, V. H.: Validation of TES methane with HIPPO aircraft observations: implications for inverse modeling of methane sources, Atmos. Chem. Phys., 12, 1823–1832, doi:10.5194/acp-12-1823-2012, 2012.

Weibring, P., Richter, D., Walega, J. G., Rippe, L., and Fried, A.: Difference frequency generation spectrometer for simultaneous multispecies detection, Opt. Express, 18, 27670–27681, doi:10.1364/OE.18.027670, 2010.

Werle, P.: Accuracy and precision of laser spectrometers for trace gas sensing in the presence of optical fringes and atmospheric turbulence, Appl. Phys. B, 102, 313–329, doi:10.1007/s00340-010-4165-9, 2011.

Werle, P. and Kormann, R.: Fast chemical sensor for eddy-correlation measurements of methane emissions from rice paddy fields, Appl. Optics, 40, 846–858, 2001.

Werle, P., Mazzinghi, P., D'Amato, F., Rosa, M. D., Maurer, K., and Slemr, F.: Signal processing and calibration procedures for in situ diode-laser absorption spectroscopy, Spectrochim. Acta A, 60, 1685–1705, 2004.

Worden, J., Kulawik, S., Frankenberg, C., Payne, V., Bowman, K., Cady-Peirara, K., Wecht, K., Lee, J.-E., and Noone, D.: Profiles of CH_4, HDO, H_2O, and N_2O with improved lower tropospheric vertical resolution from Aura TES radiances, Atmos. Meas. Tech., 5, 397–411, doi:10.5194/amt-5-397-2012, 2012.

Xiong, X., Barnet, C. D., Zhuang, Q., Machida, T., Sweeney, C., and Patra, P. K.: Mid-upper tropospheric methane in the high Northern Hemisphere: Spaceborne observations by AIRS, aircraft measurements, and model simulations, J. Geophys. Res., 115, D19309, doi:10.1029/2009JD013796, 2010.

Zahn, A. and Brenninkmeijer, C. A.: New Directions: A Chemical Tropopause Defined, Atmos. Environ., 37, 439–440, doi:10.1016/S1352-2310(02)00901-9, 2003.

Zahn, A., Weppner, J., Widmann, H., Schlote-Holubek, K., Burger, B., Kühner, T., and Franke, H.: A fast and precise chemiluminescence ozone detector for eddy flux and airborne application, Atmos. Meas. Tech., 5, 363–375, doi:10.5194/amt-5-363-2012, 2012.